Beam Splitting Planar Inverted-F Antenna for 5G Communication

Akhilesh Verma and N.S. Raghava[*]

Department of Electronics and Communication Engineering, Delhi Technological University, Delhi - 110 042, India
[*]E-mail: nsraghava@dtu.ac.in

ABSTRACT

A planar inverted-F antenna with symmetrical split beams and loaded with radio frequency absorbers (here Eccosorb MCS) for 5G communication is proposed. The multi-beam antennas reduce the requirement of number of antennas and provide wide coverage. But they require a complex system such as a phased array or MIMO antennas. On the other hand, multi-beam antennas do not have such requirements. In this work, we propose a PIFA antenna which achieves multi-beam behaviour by six slabs of absorbers placed periodically between the PIFA patch and substrate to split the beams into two directions at $\pm26°$. The proposed antenna obtains a frequency band of 24.2-25.7 GHz and achieves a high gain of approximately 10 dB at $\pm26°$. The performance of the proposed antenna is suitable for G communication. All simulations of the antenna are carried out using Ansys HFSS. The design was validated by simulations and later confirmed with measurements.

Keywords: Eccosorb MCS; Absorber; Beam split; PIFA; 5G; mm-wave

1. INTRODUCTION

The fifth generation (5G) wireless technology is required to provide high network coverage, continuous network connectivity with wide bandwidth. The mm-wave band has an unused wide spectrum to overcome all wireless service issues[1-2].

The mm-wave ranging from 1-10 mm wavelength (10-100 GHz) has many limitations. The tiny wavelength wave is affected by raindrops, oxygen absorption, and line of sight during its propagation. The beamforming, beam splitting, and directive antennas are the key solutions to overcome the problems raised at mm-wave. The multibeam antenna offers independent beams in which the selected beams reduce the interference and provide the greater coverage in desired direction which is the compulsory requirement of 5G[3]. The short wavelength allows the design of antennas to be compact along with high directivity[4-5]. For the functionality of beam splitting, beam scanning, planar inverted-F antenna is one of the best choices for 5G implementation because of its low profile, compactness and ease of fabrication. Several parameters of the PIFA antenna affect its performance. The air gap between the top patch and substrate affects the return loss and bandwidth while the distance between shorting and feed controls the impedance[6-7]. Next, we discuss past research of PIFA and other antennas for 5G.

In[8], the coverage of the desired direction with beam steering capability ranges from -90° to +90° in theta plane is presented where the scanning capability is obtained by three identical subarrays of patch antennas which are fed by switching to particular subarrays. In[9], the radiation pattern at mm-wave is distorted by the scattering of the signals. Meanwhile, the damage of the patch antenna is controlled by placing conventional radome on the patch. But due to the comparable wavelength of the antenna with the radome thickness, the radiation pattern gets distorted, which reduces the radiation directivity of the antenna. The radiation pattern improvements, as well as high gain achieved by stacking of six pieces of the substrate are placed in a radome, but it also affects its reflection coefficient. A circular patch along with a parasitic circular ring is used to obtain an ultra-wideband of 3.03 GHz bandwidth in[10]. In[11], planar inverted-F antenna (PIFA) with slots having wide bandwidth ranges from 27.57-30.75GHz and peak gain of 8.3 dBi is reported. Whereas 8-element PIFA antenna arrays were used to steer the beam by varying phase shift of each element in[12]. In[13], The dimension of the substrate is 110 mm × 60 mm which is large enough for mm-wave applications. The proposed antenna comprising an array of 4*4 patch antenna is fed by the L-probe. The radiation performance and reduction of surface waves were achieved through metal strips on the soft surface structure via fences. However, high gain with a tilted beam without using an array is reported. The two L-shaped slots etched on the patch, which are fed by a single coax feed, obtain two frequency bands of 28/38 GHz. The improvement of impedance matching and the axial ratio is achieved with the optimisation of the slots[14]. However, the wide beamwidth between 100° and 125° is achieved by parasitic patches with multiple resonances and a wide bandwidth of 13%, which covers 34.1 to 38.9 GHz frequency band through multi slotted microstrip patches[15]. The radiation pattern reconfigurability in respect of broadside radiation and end-fire radiation has been achieved by rectangular slots and dielectric loading respectively. It is observed in[16], the wide bandwidth along with high gain has been achieved through high impedance surfaces (HIS),

which suppress the surface waves. The impedance bandwidth of 32% covered 2.68 GHz to 3.65 GHz band and exhibited 4.5 dBi gain value, which is higher as compared to without HIS. However, the size of the antenna is 60*60*5.77mm³, which seems to be very large for wireless portable devices. Beam splitting capability of the antenna provides high data transfer rates reported in[17-18]. In[19], split beams are achieved using digital metasurface along with a lens in which radiation in boresight direction is improved through the lens, and beam splitting is achieved through digital metasurfaces. However[20], proposed an ultra-thin polarisation beam splitter using the property of the transmissive phase gradient metasurface (TPGM). The proposed antenna achieved more than 600 MHz bandwidth. In[21], three pairs of metamaterials (MTM) arrays for 5G MIMO applications were used. The first pair of MTM arrays with high refractive index was deployed to achieve a wide beam, whereas the second pair of MTM arrays were arranged such that the single wide beam splits into dual beams at ±30°. Gain of the antenna is enhanced by using a third pair of anisotropic MTM arrays. Triple periodic dual beam microstrip leaky wave antenna is presented in[22]. Dual radiation beams with wide bandwidth directed at $\pm35°$ and -33° is reported in[23].

In this manuscript, a combination of Eccosorb MCS absorber in a slotted planar inverted-F antenna (PIFA) is presented for mm-wave applications. The periodic structure of absorber in between the patch and substrate provides split beams in the H-plane at $\pm26°$. The absorber loaded substrate reduces the surface waves, which constructively enhances the bandwidth as well as the gain of the antenna.

2. DESIGN OF SLOTTED PIFA ANTENNA

The configuration of the proposed slotted planar inverted-F antenna is shown in Fig. 1. The antenna has been designed on 1.6 mm thick RT/duroid substrate, with the dimensions of 20 mm x 10 mm and the dimensions of the patch are $0.90\lambda_o \times 0.72\lambda_o \times 0.32\lambda_o$ where λ_o is 12.24 mm for frequency of 24.5 GHz. The employed laminate has relative permittivity (ε_r) of 2.2 and a dielectric loss tangent ($\tan\delta$) of 0.0009. The thickness of the copper patch is 0.035mm. The air gap between the patch and the substrate is $0.18\lambda_o$. The shorting plate $SH_1(2mm)$ and $SH_1(10mm)$ are soldered to both ends of the radiator to the ground at distances of F_1 and F_2 from the feed position. The distance between both shorting plates and feed helps to maintain the impedance of the antenna. The top copper radiator is fed by a 2.92mm N-type connector. As shown in Fig. 1 (a), two slots ($l_s \times W_s$) are etched on the radiator, and there are also two stubs S_1, S_2 ($0.27\lambda_o \times 0.045\lambda_o$) to maintain the impedance bandwidth and the return loss.

The design equations of the PIFA antenna[24] define dimensions as:

$$L_p + W_p - W_{SH_1} - W_{SH_2} = \lambda / 4 \quad (1)$$

$$f_o = \frac{c}{4(L_p + W_p - W_{SH_1} - W_{SH_2})} \quad (2)$$

where L_p, W_p are the length and width of the top patch and W_{SH_1}, W_{SH_2} are the width of the narrow and broad shorting plate respectively. c is the speed of light and λ is the wavelength of the desired resonant frequency (24.5 GHz).

The optimised parameters of the proposed antenna are shown in Fig. 1 are $L_p = 0.90\lambda_o$, $W_p = 0.72\lambda_o$, $W = 10mm$, $X_1 = 3mm$, $X_2 = 2mm$, $a = 2mm$, $X_4 = 3mm$, $W_s = 1.5mm$, $l_s = 6mm$, $t = 2.5mm$, $F_1 = 6.4mm$, $F_1 = 8.6mm$, $L = 20mm$ respectively.

3. DESIGN AND PARAMETRIC ANALYSIS OF BEAM SPLITTING ANTENNA

The split beam absorber loaded PIFA antenna configuration is shown in Fig. 2. The Eccosorb MCS absorber from Laird Technologies, Inc. has high permittivity, ε_r of 15 which reduces the overall voltage standing wave ratio (VSWR). This material is designed for the suppression of surface currents over a wide range of frequencies. In MIMO configuration, this material plays a very good role to reduce the RF coupling. The conventional normal RF absorbers do not have good response at high frequency. So, for high frequency, high performance absorbers are needed and the Eccosorb MCS serves the purpose. Eccosorb absorber is a highly lossy, flexible,
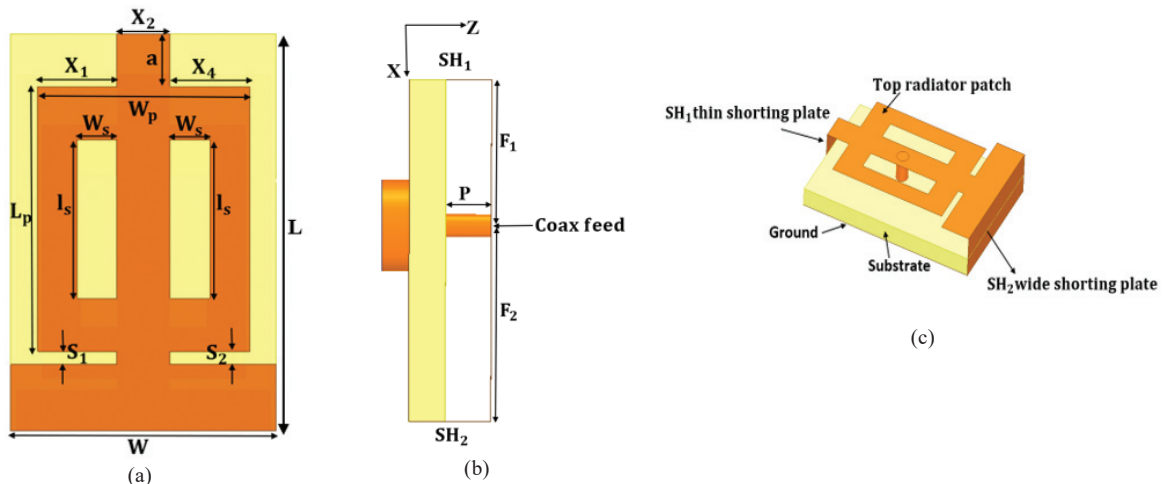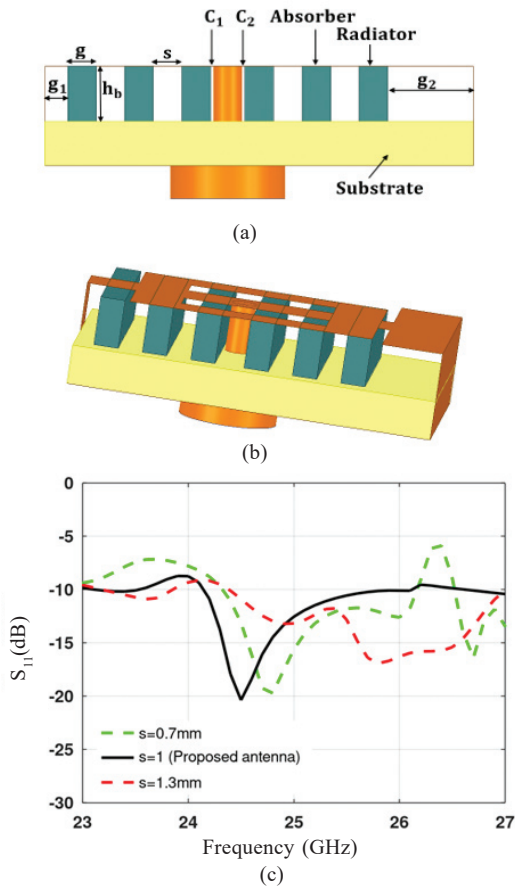

Figure 1. Geometry of the proposed slotted PIFA antenna (a) top view of the slotted patch; (b) side view, and (c) 3D view of the antenna.

(a)

(b)

(c)

Figure 2. Geometry of the proposed beam splitting antenna (a) side view; (b) 3D view ($g_1 = 0.8$, $g = 1$, $h_b = 2$, $C_1 = C_2 = 0.1$, $g_2 = 3$, units in mm), and (c) parametric analysis of the proposed antenna.

nonconductive broadband silicone absorber. In the antenna structure, six strips of the Eccosorb MCS absorber are placed periodically between the substrate and radiator. The bottom part of the absorber is touched to the surface of the substrate and the upper part of the absorber is touched to the radiator. The separation distance between all absorbers is 1 mm denoted by 's' which plays a significant role in achieving split beams and the height of the absorber is denoted by h_b . The width of the absorber is denoted by g and the gap g_1 is in between narrow shorting plate and absorber. The gap between the wide width shorting plate and the absorber is g_2 . The overall size of the beam splitting antenna is $3.2\lambda_o \times 2.5\lambda_o \times 1.2\lambda_o$.

The parametric analysis performed on the gap 's' between the absorbers of the antenna is shown in Fig. 2 (c). The value of s is increased from 0.7 mm to 1.3 mm with a step size of 0.3 mm. It can be seen that the optimised value of s is 1 mm which gives good return loss and bandwidth. The parametric analysis is carried out with high frequency structure simulator (HFSS) software.

4. BEAM SPLITTING TECHNIQUE
4.1 Theory of Beam Splitting

In this section, to get a better understanding of beam splitting behaviour of the antenna, numerical equations are derived and are discussed below.

When the absorber is embedded periodically in between the patch and substrate with equal distance, the size of the antenna is reduced in accordance with the decreased wavelength as:

$$\lambda_g = \frac{c}{f\sqrt{\varepsilon_r}} = 3.16mm \qquad (3)$$

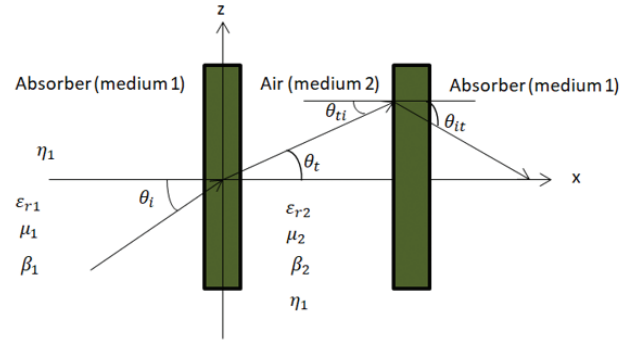whereas,

$$\varepsilon_{r1} = 15, \mu_1 = 1, \varepsilon_{r2} = 1, \mu_2 = 1 \qquad (4)$$
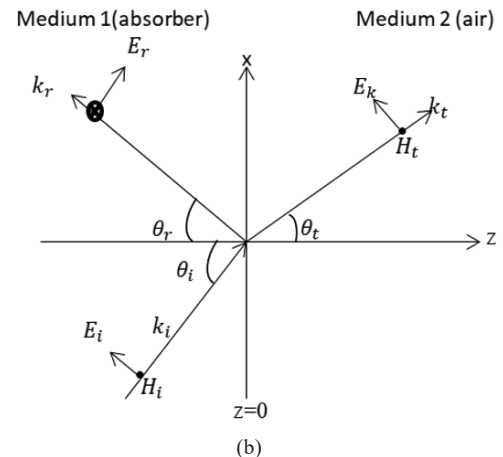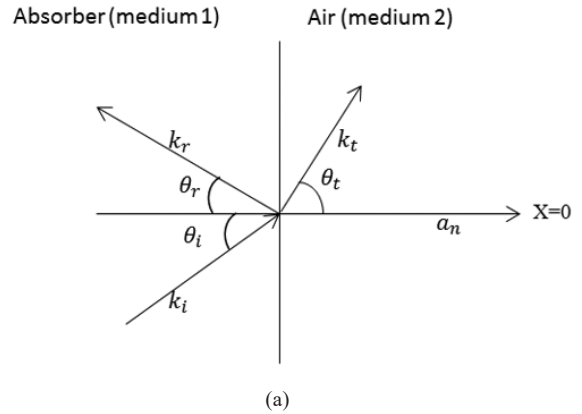
For $\theta_t = 26°$, θ_{ti} is found to be 6.48° as shown in Fig. 3.

Figures 4(a) and 4(b) show that the two cases of the propagation are obtained:

Case (i) oblique incidence and reflection of a plane wave.

Case (ii) for parallel polarisation.

Figure 3. Propagation of electric fields through different media.

(a)

(b)

Figure 4. (a) Plane wave incident and reflection and (b) Parallel polarisation of electromagnetic waves.

Oblique incidence and reflection of a plane wave as shown in Fig. 4.

where a_n is the plane of incidence, θ_i is the angle of incidence between k and a_n. As shown in Fig. 4(a), it seems that incident and reflected waves are in medium 1 and transmitted or refracted wave is in medium 2.

The incident electric field is given as

$$E_{i1} = E_o e^{-\alpha z} \cos(\omega t - \beta_1 z + \theta_i + 180°) \tag{5}$$

In Eqn (3), 180° phase shift is added because the electric field is incident from dense media to rare media.

The reflected wave is given by,

$$E_{r1} = \Gamma E_{i1}$$

$$E_i = \Gamma E_o e^{-\alpha z} \cos(\omega t - \beta_1 z + \theta_i + 180°) \tag{6}$$

where $\theta_i = 6.48°, \beta_1 = 0.13, z = 0.001m$

$$E_{i1} = E_o e^{-0.001\alpha} \cos(\omega t - 186.4°) \tag{7}$$

The reflected electric field is calculated with the help of the relation given below,

$$E_{r1} = \Gamma E_i$$

where Γ is the reflection coefficient which is computed using

$$\Gamma = \frac{\sqrt{\varepsilon_{r1}} - \sqrt{\varepsilon_{r2}}}{\sqrt{\varepsilon_{r1}} + \sqrt{\varepsilon_{r2}}} = 0.589$$

and $\qquad\qquad\qquad\qquad\qquad\qquad$ (8)

$$E_{r1} = \Gamma E_{i1}$$

$$E_{r1} = 0.589(E_o e^{-0.001\alpha} \cos \cos(\omega t - 186.4°) \tag{9}$$

The transmitted electric field is given as

$$E_{t1} = E_{to} e^{-\alpha z} \cos(\omega t - \beta_2 z + \theta_t + 180°) \tag{10}$$

here, $z = 0.002m, \beta_2 = 0.152, \theta_t = 26°$

$$E_{t1} = E_{to} e^{-0.002\alpha} \cos(\omega t - 205.9°) \tag{11}$$

$$E_{i2} = E_o e^{-0.002\alpha} \cos \cos(\omega t + 6.47°) \tag{12}$$

When the wave propagates from medium 2 (air) to medium 1 (absorber),

$$\theta_i = \theta_t = 6.48°, z = 0.001m \tag{13}$$

$$E_{i2} = E_{t1} \tag{14}$$

$$E_{r2} = \Gamma' E_{i2} \tag{15}$$

where,

$$\Gamma' = \frac{\sqrt{\varepsilon_{r2}} - \sqrt{\varepsilon_{r1}}}{\sqrt{\varepsilon_{r2}} + \sqrt{\varepsilon_{r1}}} = -0.589 \tag{16}$$

$$E_{r2} = -0.589 E_o e^{-0.001\alpha} \cos(\omega t + 25.9°) \tag{17}$$

$$E_{t2} = E_{to} e^{-\alpha z} \cos(\omega t - \beta_2 z' + \theta_t^{"}) \tag{18}$$

here, $z' = 0.002m, \theta_t^{"} = 6.48°$

$$E_{t2} = E_{to} e^{-0.002\alpha} \cos(\omega t + 6.47°) \tag{19}$$

The total incident wave is given as

$$E_i = E_{i1} + E_{i2} \tag{20}$$

$$E_i = E_o e^{-0.001\alpha} (\omega t - 186.4°) + E_o e^{-0.002\alpha} \cos(\omega t + 6.47°)$$

The total transmitted wave is given as

$$E_t = E_{t1} + E_{t2} \tag{21}$$

$$E_t = E_{to} e^{e - 0.002\alpha} \cos \cos(\omega t - 205.9°) + E_{to} e^{-0.002\alpha} \cos(\omega t + 6.47°)$$

The total reflected wave is given as

$$E_r = E_{r1} + E_{r2} \tag{22}$$

$$E_r = 0.589[E_o e^{-0.001\alpha} \cos \cos(\omega t - 186.4°] - 0.589 E_o e^{-0.001\alpha} \cos(\omega t + 25.9°)$$

Figure 4(b) depicts the parallel polarisation of electromagnetic waves.

$$E_{is} = E_{io}(\cos\theta_i a_x - \sin\theta_i a_z)e^{-j\beta_1(x\sin\theta_1 + z\cos\theta_i)} \tag{23}$$

where as $\theta_i = 6.48°, \theta_t = 26°, \beta_1 = 0.13, \beta_2 = 0.512$

$\eta_1 = 97\Omega, \eta_1 = 377\Omega, x = 0.002m, z = 0.001m$

$$E_{is} = E_{io}(a_x - 0.112a_z)e^{-0.000289j} \tag{24}$$

$$H_{is} = \frac{E_{io}}{\eta_1} e^{-j\beta_1(x\sin\theta_i + z\cos\theta_i)} a_y \tag{25}$$

$$H_{is} = 0.01E_{io} e^{-0.000289} a_z \tag{26}$$

$$E_{rs} = E_{ro}(\cos\theta_r a_x + \sin\theta_r a_z)e^{-j\beta_1(x\sin\theta_r - z\cos\theta_r)} \tag{27}$$

$$E_{rs} = E_{ro}(a_x + 0.112a_z)e^{9.88\times10^{-5}j} \tag{28}$$

The transmitted electric field in medium 2 (air) is given by

$$E_{ts} = E_{to}(\cos\theta_t a_t - \sin\theta_t a_z)e^{-j\beta_2(x\sin\theta_t + z\cos\theta_t)} \tag{29}$$

where as $\theta_t = 26°, \beta_2 = 1, x = 0.002m, z = 0.002m$

$$E_{ts} = E_{to}(0.89a_x - 0.43a_z)e^{0.0025j} \tag{30}$$

$$H_{ts} = \frac{E_{ts}}{\eta_2} e^{-j\beta(x\sin\theta_t + z\cos\theta_t)} a_y \tag{31}$$

$$H_{ts} = 0.0026E_{to} e^{-0.0012j} \tag{32}$$

The parallel polarisation reflection coefficient is given by

$$\Gamma_{11} = \frac{\eta_2\cos\theta_t - \eta_1\cos\theta_i}{\eta_2\cos\theta_t + \eta_1\cos\theta_i} = 0.47. \tag{33}$$

where

$$E_{ro} = \Gamma_{11} E_{io} \tag{34}$$

$$E_{ro} = 0.47 E_{io} \tag{35}$$

The expression for propagation constant for the parallel polarisation is given as

$$\tau_{11} = \frac{E_{to}}{E_{io}} = \frac{2\eta_2\cos\theta_i}{\eta_2\cos\theta_t + \eta_1\cos\theta_i} = 1.63 \tag{36}$$

5. RESULTS AND DISCUSSION

The fabricated prototype of the proposed beam splitting slotted PIFA antenna is shown in Fig. 5. The thickness of the absorber, the number of strips and the gap between them are optimised as discussed earlier.

5.1 3D E-field of the Beam Splitting Antenna

The electric field distribution of the patch which changes the direction and propagation of the field in the absorber is
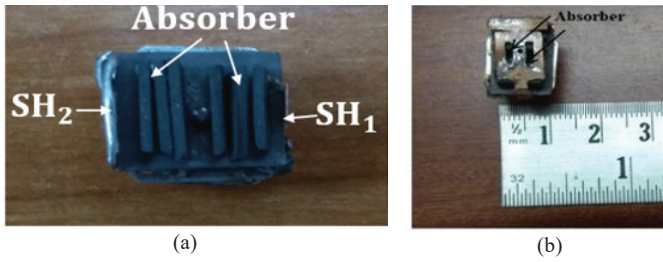
Figure 5. Fabricated beam splitting antenna (a) cross section and (b) top view.

depicted in Fig. 6. It can be seen that the electric field is diverted into two directions and the current path has also changed which gives the maximum radiation into two directions. However, in the middle of the patch near to the feed position, the current is very less, which gives a deep null in boresight direction. The absorber produces constructive interference in two different directions giving rise to two split beams. The pair of vertically placed absorber slabs toward the wide shorting plate near feed position have more electric field in two different directions that produce the split beams at $\pm26°$.

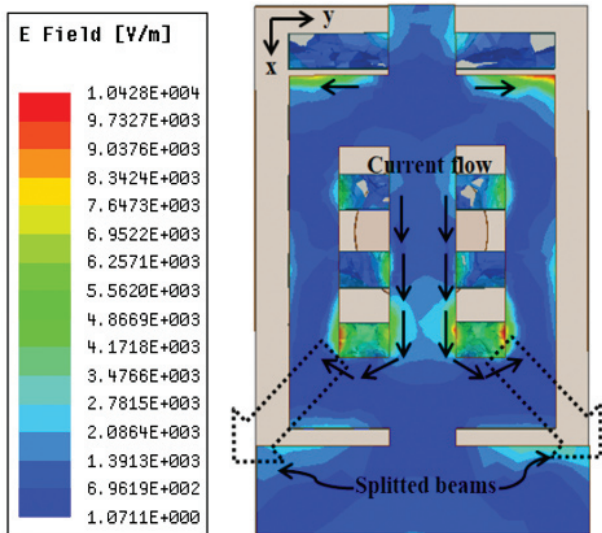**Figure 6. E-field distribution beneath the patch (in absorber) and surface current density on the radiator of beam splitting antenna at 24.5 GHz.**

5.2 S-parameter

The reflection coefficient of the beam splitting antenna is measured by R & S ZNB 40 vector network analyzer. The measured and simulated S_{11} of the antenna are illustrated in Fig. 7. The simulated S_{11} of the antenna has an impedance bandwidth of 8% in the frequency bands of 24.11-26.09 GHz. It can be seen that the measured $S11 < -10$ dB in the frequency bands of 24.2-25.7 GHz and has an impedance bandwidth of 6%.

5.3 GAIN

The beam splitting antenna provides peak gain of 10.3 dB at 24.5 GHz. Figure 8 shows good agreements between simulated and measured results for beam splitting antenna.
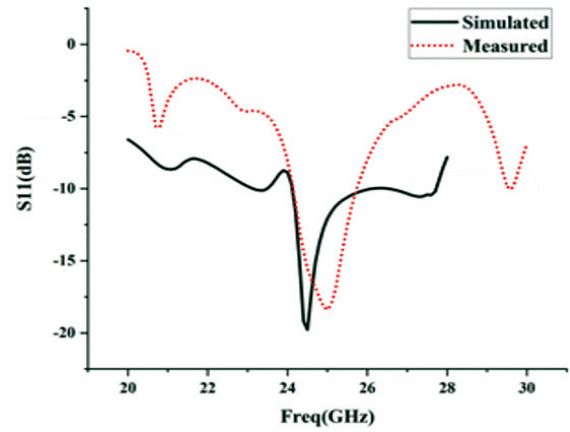

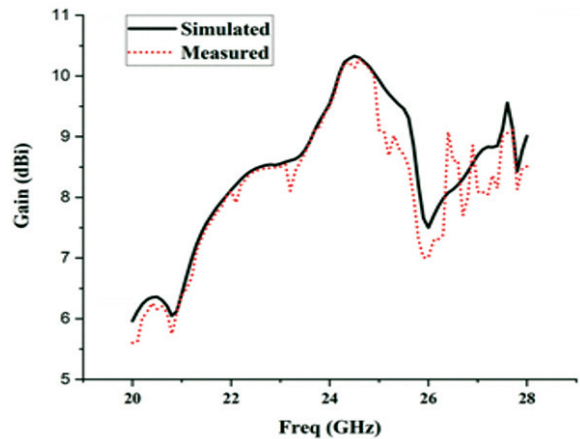**Figure 7. Simulated and measured S_{11} of the proposed beam splitting antenna.**

Figure 8. Gain of the proposed beam splitting antenna.

5.4 Radiation Patterns

The simulated and measured co and cross polarisation pattern of the proposed beam splitting antenna is depicted in Fig. 9. A deep null is observed in broadside direction and the maximum gain is obtained at $\pm26°$. The half power beam width (HPBW) of 28° and first null beam width (FNBW) is found to be 52.82°.

5.5 Beam Splitting over the Frequency Band

To get better insights, Fig. 10 shows the 2D radiation patterns of the proposed antenna at different frequencies. It can be seen from Fig. 10 that the antenna achieves beam splitting over the desired frequency band.
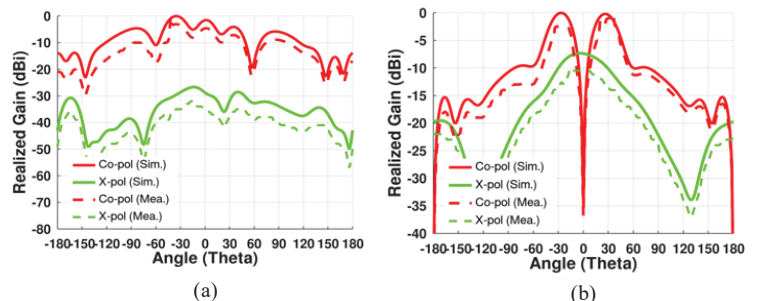

Figure 9. Simulated and measured radiation patterns at 24.5° GHz. (a) φ= 0° cut (b) φ= 90° cut.

Table 1 Comparison of the proposed antenna with previously reported work.

Ref	Freq. Band (GHz)	BW (GHz)	Size (mm³)	Gain (dBi)	Beam split	Elements
[8]	21.5	1	$110 \times 55 \times 4.5$ $11.5\lambda_o \times 5.7\lambda_o \times 0.47\lambda_o$	12.5	Yes	8
[13]	28	26.9-29	$30 \times 19.9 \times 0.79$ $4.2\lambda_o \times 2.76\lambda_o \times 0.11\lambda_o$	7.4	Yes	1
[19]	11	10.42-11.22	$53.9 \times 53.9 \times 1.57$ $2.92\lambda_o \times 2.92\lambda_o \times 0.8\lambda_o$	18.6	Yes	32
[20]	10	0.6	$256 \times 256 \times 3$ $13.6\lambda_o \times 13.6\lambda_o \times 0.16\lambda_o$	-	Yes	Multiple
[21]	26	24.25-27.5	$30 \times 30.5 \times 0.508$ $4\lambda_o \times 3.91\lambda_o \times 0.065\lambda_o$	7.4	Yes	MIMO
[23]	5.5	5.18-5.8	$67 \times 74 \times 3.175$ $1.22\lambda_o \times 1.35\lambda_o \times 0.058\lambda_o$	7.92 at 35° & 5.94 at -33°	Yes	1
Work	24.5	24.2-26.1	$10 \times 8 \times 3.6$ $3.2\lambda_o \times 2.5\lambda_o \times 1.2\lambda_o$	**10.07** at -26° & 10.3 at +26°	**Yes**	1
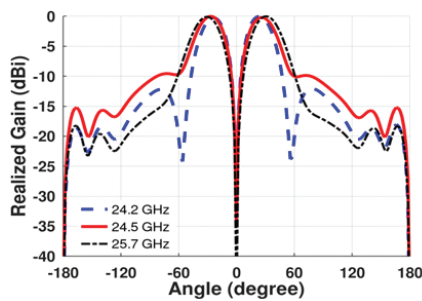
Figure 10. Beam splitting at different frequencies.

5.6 Performance of Proposed Work

Table 1 shows the comparison between the proposed antenna and the previously published works in literature.

The presented antenna provides a better impedance bandwidth along with beam splitting. It offers compact size with good gain throughout the band compared with existing structures.

6. CONCLUSION

This paper proposed a beam splitting antenna in which six slabs of absorbers are periodically placed between the patch and substrate. Placing of the absorber at optimised locations showed beam splitting with two beams in directions of -26° and +26° with a deep null in the broadside direction. The measured results show that the beam splitting antenna has realised a bandwidth of 6% with a maximum gain of 10.3 dBi respectively. With these characteristics, the proposed antenna can be a good candidate for 5G applications.

REFERENCES

1. Wells, J. Faster than fiber: The future of multi-Gb/s wireless. *IEEE Microw. Mag.*, 2009, **10**(3), 104-12.
   doi: 10.1109/MMM.2009.932081

2. Shorbagy, M.E.; Shubair, R M.; AlHajri, M. I. & Mallat, N.K. On the design of millimetre-wave antennas for 5G. *In* Mediterranean Microwave Symposium (MMS), 2016.
   doi: 10.1109/MMS.2016.7803878

3. Kirthiga, S. & Jayakumar, M. Performance of dualbeam MIMO for millimeter wave indoor communication systems. *Wirel. Personal Commun.*, 2014, **77**(1), 289-307.
   doi: 10.1007/s11277-013-1506-0

4. Rappaport, T.S.; Gutierrez, F.; Ben-Dor, E.; Murdock, J.N.; Qiao, Y. & Tamir, J.I. Broadband millimeter-wave propagation measurements and models using adaptive-beam antennas for outdoor urban cellular communications. *IEEE Trans. Antennas Propag.*, 2013, **61**(4), 1850-59.
   doi: 10.1109/TAP.2012.2235056

5. Chu, H. & Guo, Y.X. A filtering dual-polarized antenna subarray targeting for base stations in millimeter-wave 5g wireless communications. *IEEE Trans. Compon. Packaging Manuf. Technol.*, 2017, **7**(6), 964-73.
   doi: 10.1109/TCPMT.2017.2694848

6. Chattha, H.T.; Huang, Y. & Lu, Y. PIFA bandwidth enhancement by changing the widths of feed and shorting plates. *IEEE Antennas and Wirel. Propag. Lett.*, 2009, **8**, 637-40.
   doi: 10.1109/LAWP.2009.2023251

7. Ishfaq, M.K.; Abd Rahman, T.; Himdi, M.; Chattha, H.T.; Saleem, Y.; Khawaja, B.A. & Masud, F. Compact four-element phased antenna array for 5G applications. *IEEE Access*, 2019, **7**, 161103-111.
   doi: 10.1109/ACCESS.2019.2949149

8. Ojaroudiparchin, N.; Shen, M.; Zhang, S. & Pedersen, G.F. A Switchable 3-D-Coverage-Phased Array Antenna Package for 5G Mobile Terminals. *IEEE Antennas Wirel. Propag. Lett.*, 2016, **15**, 1747-50.
   doi: 10.1109/LAWP.2016.2532607

9. Hong, K.D.; Huang, G.L.; Zhang, X. & Yuan, T.A. A High-Performance Radome for Millimeter Wave Antenna Applications. Cross Strait Quad-Regional Radio Science and Wireless Technology Conference (CSQRWC), July 2019, Taiyuan, China.
doi: 10.1109/CSQRWC.2019.8799352

10. Raghava, N.S.; De, A.; Arora, P.; Malhotra, S.; Bazaz, R.; Kapur, S. & Manocha, R. A novel patch antenna for ultra wideband applications. *In* IEEE International Conference on Communications and Signal Processing, 2011, 276-79.
doi: 10.1109/ICCSP.2011.5739318

11. Morshed, K.M.; Esselle, K.P.; Heimlich, M.; Habibi, D. & Ahmad, I. Wideband slotted planar inverted-F antenna for millimeter-wave 5G mobile devices. *In* IEEE Region 10 Symposium (TENSYMP), 2016, 194-97.
doi: 10.1109/TENCONSpring.2016.7519403

12. Stanley, M.; Huang, Y.; Loh, T.; Xu, Q.; Wang, H. & Zhou, H. A high gain steerable millimeter-wave antenna array for 5G smartphone applications. IEEE European Conference on Antennas and Propagation (EUCAP), 2017, 1311-14.
doi: 10.23919/EuCAP.2017.7928542

13. Park, J.S.; Ko, J.B.; Kwon, H.K.; Kang, B.S.; Park, B. & Kim, D. A Tilted Combined Beam Antenna for 5G Communications Using a 28-GHz Band. *IEEE Antennas Wirel. Propag. Lett.*, 2016, **15,** 1685-88.
doi: 10.1109/LAWP.2016.2523514

14. Aliakbari, H.; Abdipour, A., Mirzavand, R., Costanzo, A., & Mousavi, P. A single feed dual-band circularly polarized millimeter-wave antenna for 5G communication. *In* 10th European Conference on Antennas and Propagation (EuCAP), April 2016, 1-5.
doi: 10.1109/EuCAP.2016.7481318

15. Kornprobst, J.; Wang, K.; Hamberger, G. & Eibert, T.F. A mm-wave patch antenna with broad bandwidth and a wide angular range. *IEEE Trans. Antennas Propag.*, 2017, **65**(8), 4293-98.
doi: 10.1109/TAP.2017.2710261

16. Panda, P K. & Ghosh D. Wideband and high gain tuning fork shaped monopole antenna using high impedance surface. *Int. J. Electron. Commun. (AEÜ).*, 2019, **111**, 84-90.
doi: 10.1016/j.aeue.2019.152920

17. Korta, L.B. & Seaks, C.E. Split beam antenna apparatus for developing angularly oriented beams', 1975, US Patent 3,911,443A.

18. Teillet, A. Multiband 40 degree split beam antenna for wireless network', 2013, US Patent US 2013/0285852 A1.

19. Katare, K.K.; Chandravanshi, S.; Biswas, A. & Akhtar, M.J. Realization of split beam antenna using transmission-type coding metasurface and planar lens. *IEEE Trans. Antennas Propag.*, 2017, **67**(4), 2074-84.
doi: 10.1109/TAP.2019.2891755

20. Cai, T.; Wang, G.M.; Zhang, X.F.; Liang, J.G.; Zhuang, Y.Q.; Liu, D. & Xu, H.X. Ultra-thin polarization beam splitter using 2-D transmissive phase gradient metasurface. *IEEE Trans. Antennas Propag.*, 2017, **63**(12), 5629-36.
doi: 10.1109/TAP.2015.2496115

21. Jiang, H.; Si, L.M.; Hu, W. & Lv, X. A symmetrical dual-beam bowtie antenna with gain enhancement using metamaterial for 5G MIMO applications. *IEEE Photonics J.*, 2019, **11**(1), 1-9.
doi: 10.1109/JPHOT.2019.2891003

22. Ma, Z.L. & Jiang, L.J. One-dimensional triple periodic dual-beam microstrip leaky-wave antenna. *IEEE Antennas Wirel. Propag. Lett.*, 2014, **14**, 390-93.
doi: 10.1109/LAWP.2014.2365394

23. Khidre, A.; Lee, K.F.; Elsherbeni, A.Z. & Yang, F. Wide band dual-beam U-slot microstrip antenna. *IEEE Trans. Antennas Propag.*, 2013, **61**(3), 1415-18.
doi: 10.1109/TAP.2012.2228617

24. Kumar, N. & Khanna, R. A compact multi-band multi-input multi-output antenna for 4G/5G and IoT devices using theory of characteristic modes. *Int. J. RF Microwave Comput. Aided Eng.,* 2020, **30**(1), 22012.
doi: 10.1002/mmce.22012

25. Sadiku, M.N. *Elements of electromagnetics*. Oxford university press, 2014. 455 p.

CONTRIBUTORS

Mr Akhilesh Verma received Master's in Electronics and Communication Engineering from the National Institute of Technical Teachers' Training and Research, Chandigarh, India in 2014. He has been working toward his PhD at Delhi Technological University, Delhi, since 2016. He has authored or co-authored more than 12 articles in peer reviewed journals and conference proceedings. He has also published one Indian patent. His research interests include mm-wave antennas, Beamforming networks, Passive phase shifters, SIW for mobile terminals and base stations.
In the current study, he developed theory, design, and performed simulations using HFSS.

Prof. N.S. Raghava is working as a professor in Electronics and Communication Engineering Department (H.O.D) in Delhi Technological University, India. He has authored or co-authored more than 80 articles in peer reviewed journals and conference proceedings. He has also published two Indian patents. His area of specialisation is Antenna and Propagation, Microwave Engineering, Digital Communication, Wireless comm., Cloud Computing, Information Security.
In the current study, he verified the methods and results and supervised the findings of this work.